



## **Full Length Research Article**

### **MODELLING DEPENDENCY STRUCTURAL OF THE WIND ENERGY IN LEBANON**

**Hussein Khraibani and \*Zaher Khraibani**

Lebanese University, Faculty of Sciences, Department of Applied Mathematics, Hadat, Lebanon

#### **ARTICLE INFO**

##### **Article History:**

Received 17<sup>th</sup> October, 2016  
Received in revised form  
27<sup>th</sup> November, 2016  
Accepted 04<sup>th</sup> December, 2016  
Published online 30<sup>th</sup> January, 2017

##### **Key Words:**

Wind power,  
Times series,  
Copulas, Lebanon.

#### **ABSTRACT**

For several decades, wind power is experiencing tremendous growth, however, the production of wind energy depends on wind intensity, strongly volatile, and is therefore characterized by a high degree of uncertainty. Planning the installation of a wind farm for several stations requires the assessment of the risk which in turn results in an assessment of the variability in production. Longevity, it starts with the recognition of the links between the various stations. The objective of this article is to develop a dependency structure assessment approach between different stations in Lebanon. The database used includes daily subsistence wind speeds of fourteen stations in Lebanon over a period of 6 years, from October 28<sup>th</sup>, 2009 until March 15<sup>th</sup>, 2016 and freely available on the NOAA network of American government. This database are used to estimate the necessary models such as, the univariate time series which will be modeled by the ARIMA process. We will establish a structure of spatial dependence of the innovations of these processes between different stations by using the copulas theory.

*Copyright©2017, Hussein Khraibani and Zaher Khraibani. This is an open access article distributed under the Creative Commons Attribution License, which permits unrestricted use, distribution, and reproduction in any medium, provided the original work is properly cited.*

#### **INTRODUCTION**

The wind is a source of energy that is continually renewed by natural phenomena. Wind energy is growing in different countries of the world, growing at 30% per year. This development of the wind energy is due to the environmental qualities of this form of energy but also to other economic factors such as; speed of installation, cost predictability over the long term, energy independence, financial aid, etc. At the end of 2033, wind power represents 218,500 megawatts (MW) of installed capacity in the worldwide with a significant growth (+ 21% capacity in 2011) (Nicola Armaroli, 2011). The experts from the World Wind Energy Council predict that wind energy will continue to grow globally, particularly in emerging countries such as Brazil, India and Mexico (Fthenakis, 2009). This energy began in Egypt in the 1990s with the wind farms in Zaafarana generating 225 MW. More recently, Egypt has tendered for the construction of a 200 MW wind farm in the Gulf of El-Zayt. In Jordan, the central power generation company has set up two pilot wind farm projects: a 320 KW fleet in Ibrahimia, installed in 1988, and a 1.2 MW fleet in Hofa. In Syria, studies on wind speed have been carried out, but so far there is no large wind farm (Allen *et al.* 2008). In the literature there exists various studies on the wind energy such as the spatial dependence of the wind (Oliver Grothe *et al.*, May 2011), and the distribution of the optimal wind energy, based on the copula, in the authors modeled the marginal distribution and structure of the wind speed dependence of the regions considered, which is the first to systematically analyze wind farm networks of different sizes.

Moreover there exist a new method for generating the Wind Speed Time Series (WSTS) dependency based on copula theory and univariate time series. An Autoregressive Moving Average (ARMA) model and multivariate GARCH model are applied to represent the time series of wind speed. Through the review of literature, this article will be structured as follows. In a first part, we will see how modelling the wind speed for each associated station. Generally, univariate time series will be modeled by ARMA-GARCH type processes. Then we will choose the one that best adapts model to create a possible link between several stations. In addition we identify stations (sites) and extract the daily wind speed data for each station over a given period (from October 2009 to March 2016). After seasonal adjustment, we estimate a stationary stochastic process. The innovations of each estimated stochastic process will establish the temporal and spatial dependence between the studied stations by using the copulas theory.

**\*Corresponding author: Zaher Khraibani,**

*Lebanese University, Faculty of Sciences, Department of Applied Mathematics, Hadat, Lebanon.*

## MATERIALS AND METHODS

### Wind Energy in the World

We give in this subsection some descriptive analysis of the distribution of the wind energy in the world.

The importance of wind energy in Lebanon comes to solve the problem of the electricity sector for several years. Today, the electricity sector faces two major problems, one of a technical nature and the other of a financial nature. From a technical point of view, there is a large gap between national demands, which needs 2,400MW and supply, which is 1,500MW. Moreover, these numbers do not take into account the energy needs of the millions of Syrian refugees who were installed in Lebanon during the war in Syria. The production is mainly using the fossil fuels and the demand exceeds the supply and the breakdowns are frequent during the peak periods (Harajli *et al.*, 2011). In general, renewable energies are a response to global warming, in the Lebanese case it is also a response to electricity production.

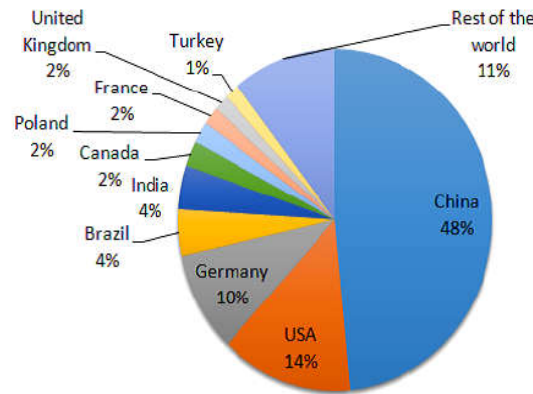


Figure 1. The first 10 countries new capacity installed between January - December 2015

Ideally, Lebanon could achieve a 50% ratio of renewable energy in 20 years, and some of this production could be provided by wind power. Certainly it would not be obvious to put wind turbines everywhere but, unlike solar energy, the wind turbine produces more power over a restricted space. If photovoltaic panels are installed in an agricultural area, agriculture is killed, while the land around the wind turbine can be exploited. In Lebanon, it is a response to local pollution, which is felt between 10 and 15km around the power stations that produce fuel oil. With wind power, the purchase price for the consumer is much lower. Wind is generally cheaper than solar, depending on the project, the difference may vary from 30% to 100%, even though this difference is now tending to fade. Finally, it is a sustainable production that consumes only wind and contributes to the country's energy independence. In 2009, at the Copenhagen summit, Lebanon had committed itself to produce 12% of its energy from renewable sources by 2020 (Al Zohbi *et al.*, 2041). It is therefore urgent for Lebanon to find a solution to cover demand with a clean energy source.

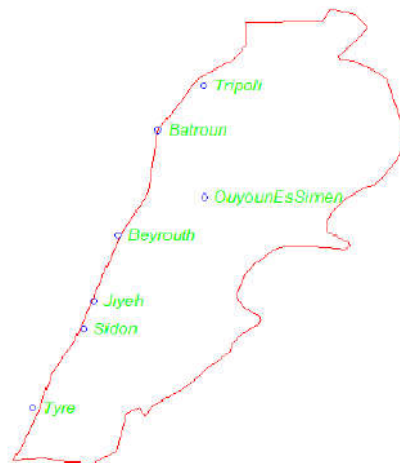


Figure 2. Geographical location of station on Lebanese territory

### Databases of the wind energy in Lebanon

The acquisition of historical databases allows one to observe first a trend of change of the wind regime over the long term. Unlike these long-term wind variations, a. The using system for the measure of wind speed is the GFS (Global Forecast System). It is calculated by the National Centers for Environmental Prediction (NCEP) a department of NOAA (National Oceanic and Atmospheric Administration), NWS (National Weather Service), USA. The data are obtained by measurements of wind speed with a frequency of 8 observations per day (one measurement every 3 hours) and then we calculated the average of the wind speed to obtain the daily wind speed in 7 stations (Figure 2), (Jiyeh, Sidon, Tyre in south of Lebanon, Beirut the Capital, Batroun and Tripoli in north of Lebanon and Ouyoun Es Simen in Mount Lebanon).

**Stochastic model**

In this subsection, we will adjust a time series model to the wind speed data for each site (Benth *et al.*, 2010), proposed the time series univariate with seasonal (ARMA) for modelling the wind speed data. The most time series have a tendency and / or a seasonal oscillation (on shorter time scales than the year) characterizes the wind in a Station, so it is more predictable. The wind regime will not be the same in winter as in summer. The selection of the station is important and the wind speed data is distributed in 14 stations in different regions in Lebanon from 28/11/2009 to 15/3/2016.

We consider a time series succession of observations over time  $\{X_t, t = 1, 2, \dots, n\}, t \in \mathbb{Z}$ .

The stationarity has an important role in the prediction of time series which possess the following conditions:

$$E(X_t) = \mu; V(X_t) = \sigma^2 = constant; cov(X_t, X_{t+h}) = \gamma_h.$$

If the series is stationary without differentiation then it is modeled by an ARMA(p, q) process. Otherwise, we perform a successive differentiations to yield the series stationary and the initial series will be modeled by an ARIMA(p, d, q) process where d is the number of differentiations necessary to obtain a stationary series (Phillips, 1988) There exist a several tests to detect the stationarity among these tests: Kwiatkowski-Phillips-Schmidt-Shin "kps" (Kwiatkowski *et al.*, 1992), augmented Dickey-Fuller "adf" (Dickey & Fuller, 1979), and the Phillips - Perron "pp". In the rest of this paper, we use the simplest and classical test, namely the augmented Dickey-Fuller test which the hypotheses test  $H_0$ : The model is non-stationary and  $H_1$ : The model is stationary. In order, the sites chosen for the article are: Jiyeh (dsj), Sidon (dssid) and Tyre (dsty) in South Lebanon, Beirut (dsb) Capital, Batroun (dsba) and Tripoli (dstr) in the North and Ouyoun Es Simen Dsouy at Mount Lebanon. However, the wind speed distributions of these sites are asymmetric and have seasonal effects, so they have to be processed and seasonally adjusted.

**Modeling and interpretation of results**

This transformation allows the obtaining of symmetric values using the Box Cox and Tukey (Box *et al.*, 1964) transformations. If the proper transformations of this series are carried out, one returns to a constant tendency in time and to a nonvolatile seasonality. Box-Cox transformation is given by the transformation formula:

$$y(\lambda) = \begin{cases} \frac{y^\lambda - 1}{\lambda} & \text{if } \lambda \neq 0 \\ \log y & \text{if } \lambda = 0 \end{cases}$$

With  $\lambda$  is a parameter estimated by the maximum likelihood method takes the values between [-2, 2]. Tukey in 1977 neatly describes re-expressing variables using a power transformation:

**Table 1. The table modified by Tukey**

$\lambda$	-2	-1	-1/2	0	1/2	1	2
y	$-\frac{1}{x^2}$	$-\frac{1}{x}$	$-\frac{1}{\sqrt{x}}$	$\log x$	$\sqrt{x}$	x	$x^2$

First it is necessary to find the best value of  $\lambda$  for each site:

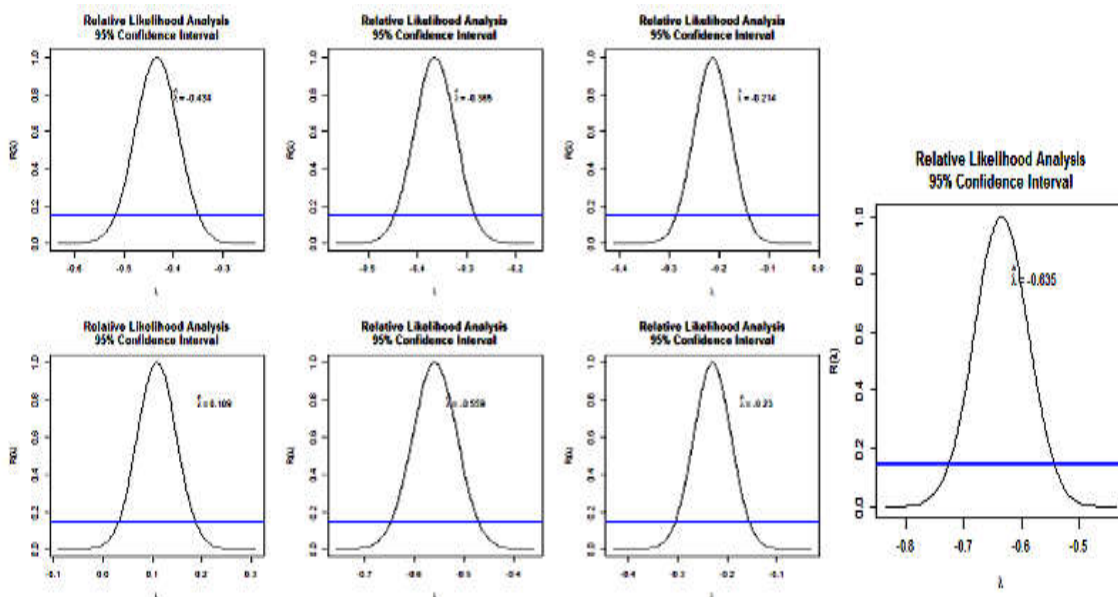


**Figure 3. Curve of the best value of  $\lambda$  for each site**

The transformation of each site:

According to the application on *R library "forecast"* we compare the different transformations for each site, so we obtain the following Table:

**Table 2. The best transformation for each site (graphically and by Skweness test)**

Station	$\lambda$	Tukey transformation	Best transformation	Skweness
Jiyeh	-0.434	$-1/\sqrt{y}$	$y = \frac{y^\lambda - 1}{\lambda}$	0.01305953
Beirut	-0.365	$-1/\sqrt{y}$	$y = \frac{y^\lambda - 1}{\lambda}$	0.01956873
Batroun	-0.214	$-1/\sqrt{y}$	$y = \frac{y^\lambda - 1}{\lambda}$	0.006445448
Ouyoun Es Siman	0.109	$Log(y)$	$y = \frac{1}{\sqrt{\lambda}}$	-0.03040134
Sidon	-0.559	$-1/\sqrt{y}$	$y = \frac{y^\lambda - 1}{\lambda}$	-0.0621482
Tripoli	-0.23	$-1/\sqrt{y}$	$y = \frac{y^\lambda - 1}{\lambda}$	0.01768482
Tyre	-0.635	$-1/\sqrt{y}$	$y = \frac{y^\lambda - 1}{\lambda}$	-0.00327468

Viewing data after transformations given by the following graphics:

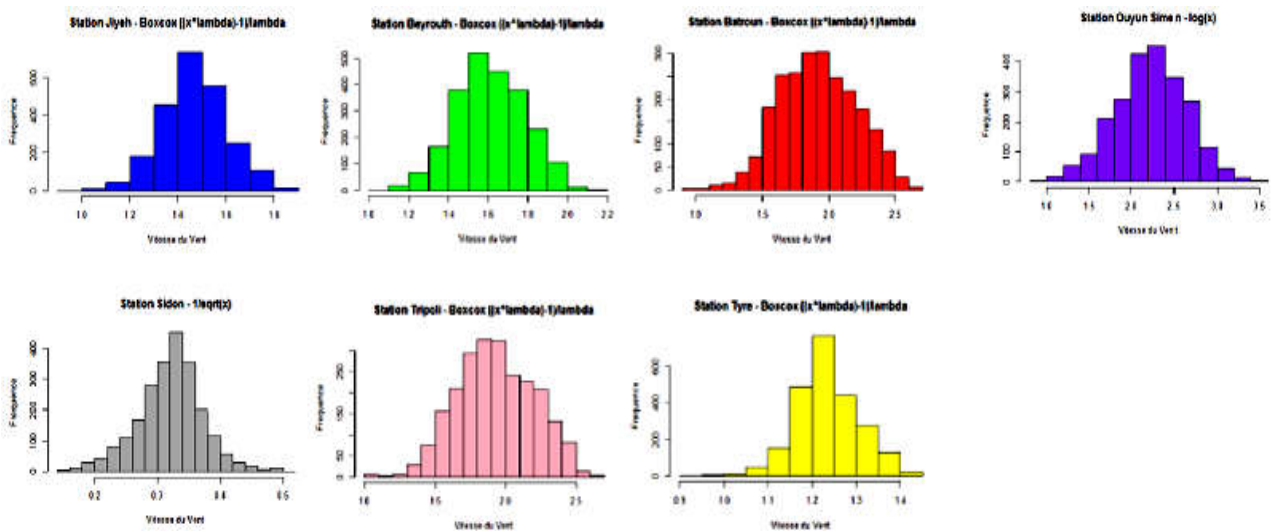


**Figure 4. Histogram of each Station after transformation**

Based on Figure 4 we see that our distributions will be almost symmetrical. Hence the hypothesis of symmetry of the data is satisfied.

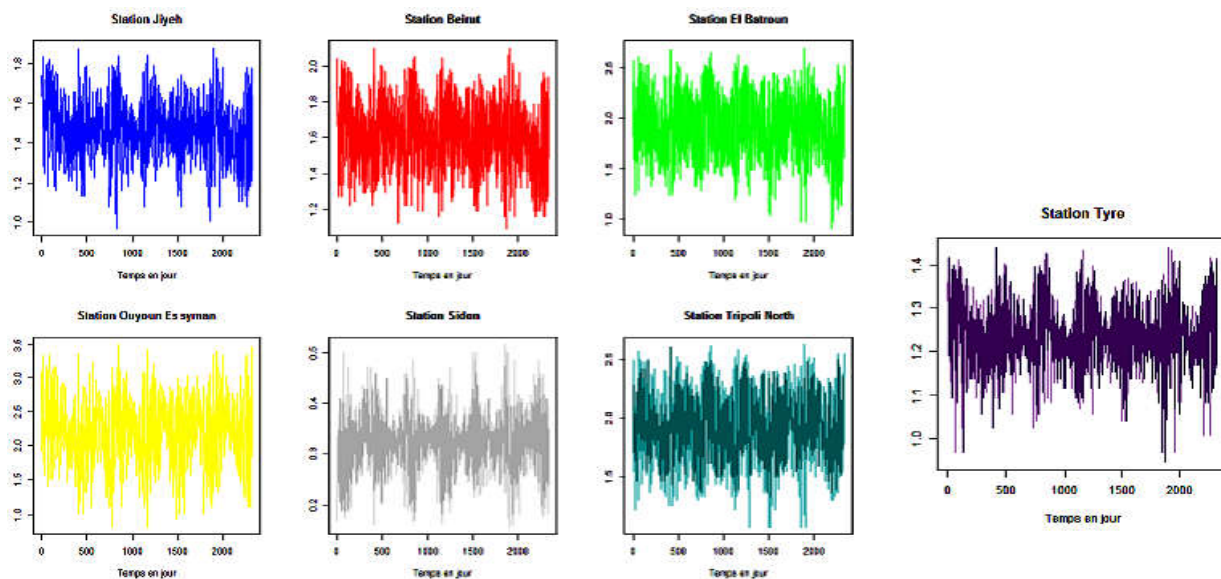


**Figure 5. Curve of the wind speed of each Station after the transformation**

From Figure 5 it is clear that there exist a seasonal effect. We recall that in this article we interested in a first time to obtain a stationary series. In a second step, we use these series to extract the innovations and then we validate the property "white noise" of these innovations. Once the validation is complete, the data will be ready to be modeled by the copulas. The transformed variable of the wind speed can therefore be expressed in the form of the equation of the following model:

$$X_t = S_t + \sum_{i=1}^p \Phi X_{t-i} + \sum_{j=1}^q \theta_k \epsilon_{t-j} + \epsilon_t$$

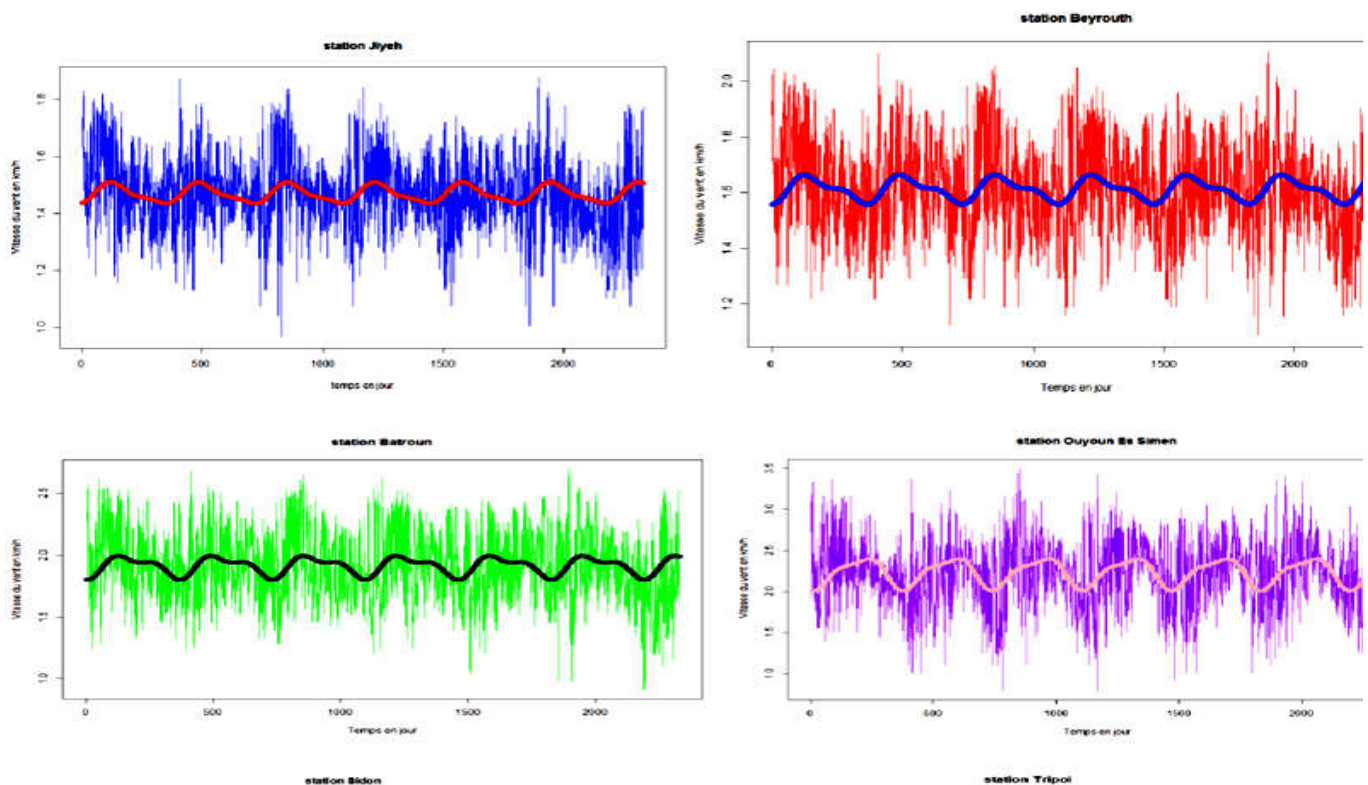
With  $\epsilon_t = \sigma_t \eta_t$ ;  $\hat{\sigma}_t^2$  is the historical mean of the variance and  $\eta_t$  is the residual. For daily data, the seasonal component  $S_t$  is calculated using the following nonlinear (periodic) model:

$$S_t = a_0 + \sum_{k=0}^1 a_{2k+1} \cos \frac{(2k+2)\pi t}{365} + \sum_{k=0}^1 a_{2k+2} \sin \frac{(2k+2)\pi t}{365}$$

The model will be applied individually on each series. The obtained residues for each series will be diagnosed by the ARCH test to be sure that there is no sequence of heteroscedasticity. In the following applications, the wind speed measurements of each station are selected from 28/10/2009 to 15/3/2016, corresponding to 7 years of observations.

**Table 3. Periodic cos series model to calculate the seasonal averages**

Site	Equation
Jiyeh	$stj = 1.470611 - 0.02243 \times \cos\left(\frac{2 \times \pi \times t}{365}\right) - 0.00931 \times \cos\left(\frac{4 \times \pi \times t}{365}\right) + 0.0244 \times \sin\left(\frac{2 \times \pi \times t}{365}\right) - 0.00573 \times \sin\left(\frac{4 \times \pi \times t}{365}\right)$
Beyrouth	$stb = 1.61228 - 0.03771 \times \cos\left(\frac{2 \times \pi \times t}{365}\right) - 0.01669 \times \cos\left(\frac{4 \times \pi \times t}{365}\right) + 0.01887 \times \sin\left(\frac{2 \times \pi \times t}{365}\right) - 0.00966 \times \sin\left(\frac{4 \times \pi \times t}{365}\right)$
Batroun	$stba = 1.91837 - 0.0757 \times \cos\left(\frac{2 \times \pi \times t}{365}\right) - 0.03759 \times \cos\left(\frac{4 \times \pi \times t}{365}\right) + 0.01627 \times \sin\left(\frac{2 \times \pi \times t}{365}\right) - 0.01386 \times \sin\left(\frac{4 \times \pi \times t}{365}\right)$
Ouyoun Es Siman	$stouy = 2.2314 - 0.16727 \times \cos\left(\frac{2 \times \pi \times t}{365}\right) - 0.05545 \times \cos\left(\frac{4 \times \pi \times t}{365}\right) - 0.06251 \times \sin\left(\frac{2 \times \pi \times t}{365}\right) - 0.0009 \times \sin\left(\frac{4 \times \pi \times t}{365}\right)$
Sidon	$stsid = 0.3263 + 0.0096 \times \cos\left(\frac{2 \times \pi \times t}{365}\right) + 0.00314 \times \cos\left(\frac{4 \times \pi \times t}{365}\right) - 0.00959 \times \sin\left(\frac{2 \times \pi \times t}{365}\right) + 0.00241 \times \sin\left(\frac{4 \times \pi \times t}{365}\right)$
Tripoli	$sttr = 1.93011 - 0.07237 \times \cos\left(\frac{2 \times \pi \times t}{365}\right) - 0.04757 \times \cos\left(\frac{4 \times \pi \times t}{365}\right) + 0.01973 \times \sin\left(\frac{2 \times \pi \times t}{365}\right) + 0.00843 \times \sin\left(\frac{4 \times \pi \times t}{365}\right)$
Tyre	$stty = 1.2352 - 0.00842 \times \cos\left(\frac{2 \times \pi \times t}{365}\right) - 0.00503 \times \cos\left(\frac{4 \times \pi \times t}{365}\right) + 0.01771 \times \sin\left(\frac{2 \times \pi \times t}{365}\right) - 0.00467 \times \sin\left(\frac{4 \times \pi \times t}{365}\right)$



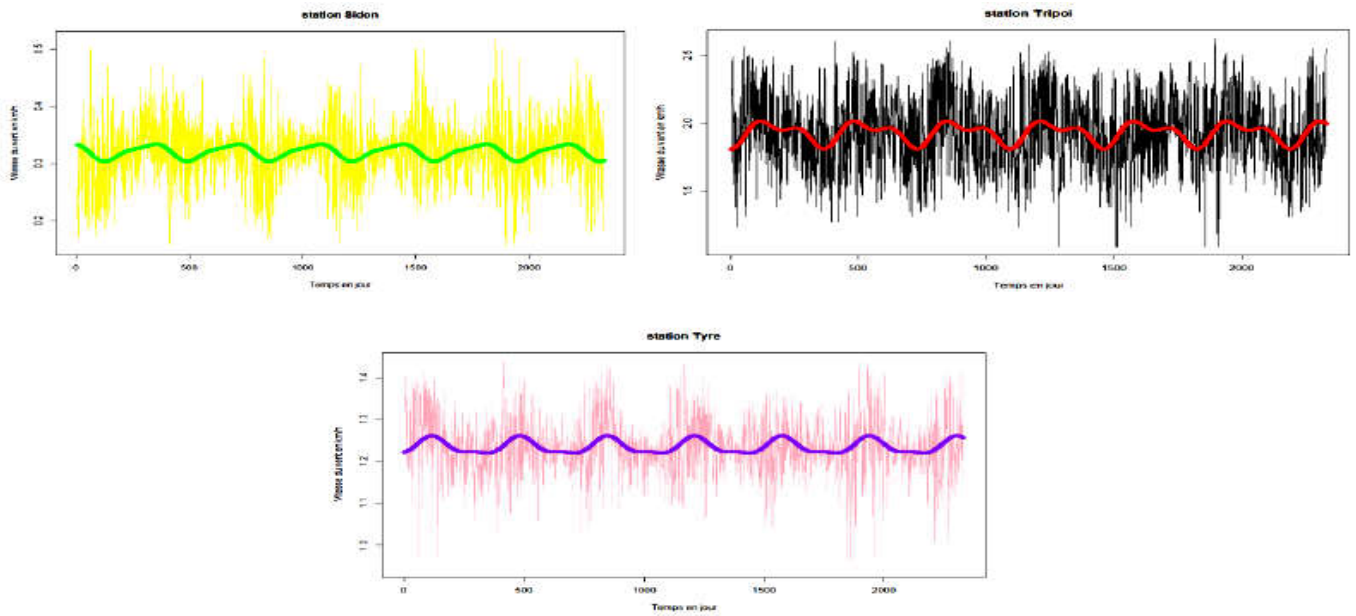


Figure 6. Wind speed curve for each station after transformation with the periodic model

Figure 6 gives the appearance of periodic models and measured wind speed data after suitable transformations, we note that for the seven sites, the periodic curves are dissimilar. In the follows we give an example for one station (Jiyeh).

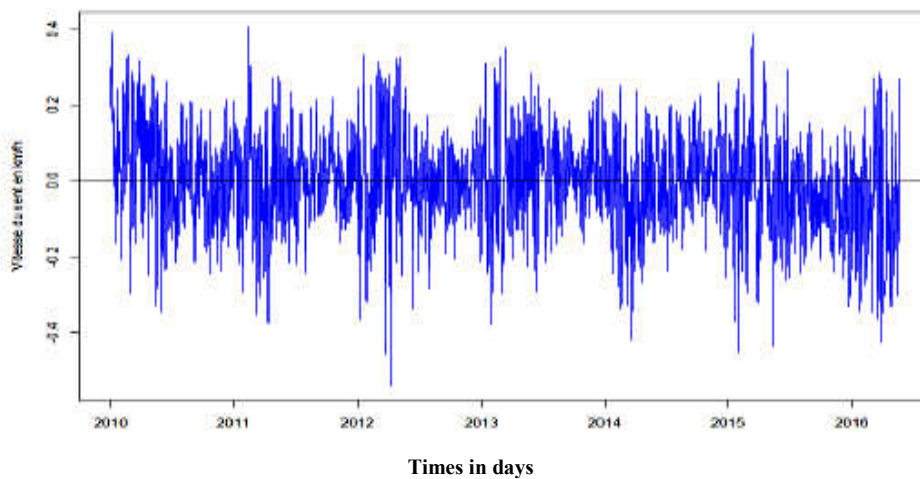


Figure 7. Seasonally adjusted data for Jiyeh station

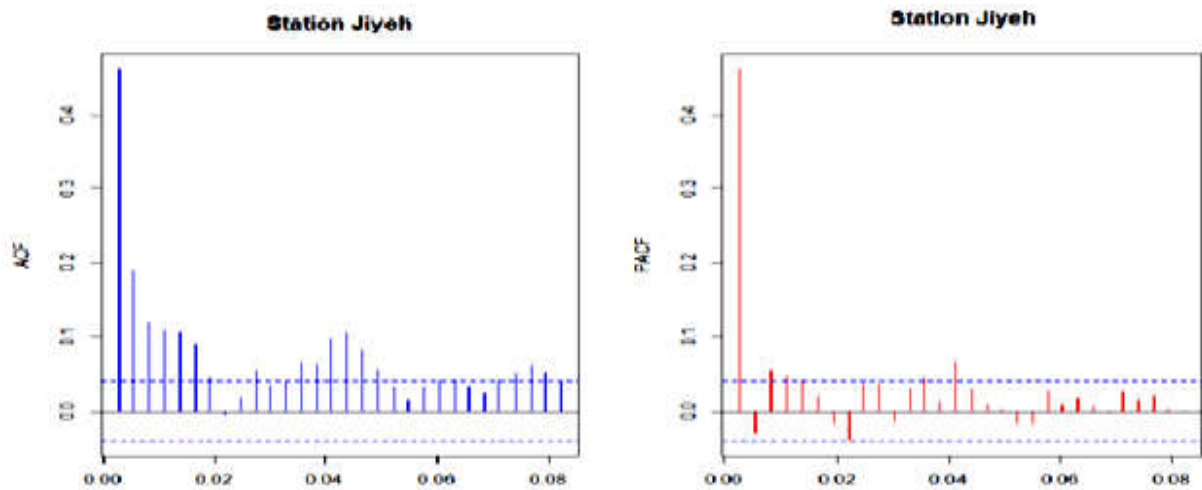


Figure 8. Autocorrelation and partial autocorrelation functions of seasonally adjusted data for Jiyeh station

Visually, we observe the non stationarity of the transformation of the data according to Figure 7 also according to the ACF and PACF. The Dickey-Fuller test confirms this result ( $p\text{-value} = 0.6816 > 0.05$ ).

**Table 4. Test of stationarity for the transformed data in Jiyeh station**

Lag	400	500	600	700	800
p-value	0.5073	0.5616	0.8942	0.7609	0.6816

We conclude that the seasonally adjusted series is non-stationary so it follows an ARIMA model and then we can make a first differentiation.

**Table 5. Test of stationarity for the seasonally adjusted data after differentiation in Jiyeh station**

Lag	100	200	300	400	500
p-Value	0.01	0.01	0.01	0.01	0.0342

After differentiation and based on the results of the Dickey-Fuller test applied over several periods of time, we obtain p-values <5%, we reject the null hypothesis of the non-stationary. So the test confirms the absence of a unit root, consequently the series became stationary.

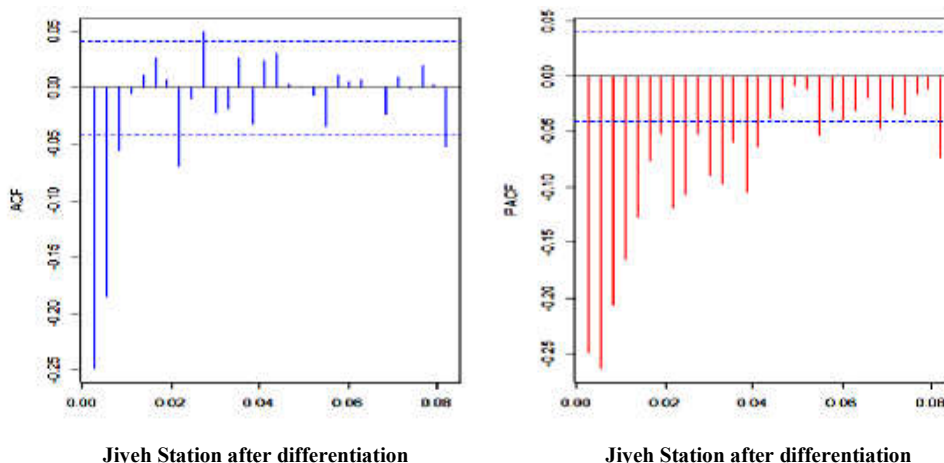


**Figure9. Autocorrelation and partial autocorrelation functions of transformed and seasonally adjusted and differentiated data (d = 1) of Jiyeh Station (dsj)**

The series (dsj) is therefore stationary, we will search an ARMA(p, q) model. To know the orders of the ARMA(p, q) model, we will use the correlogram of the stationary series (dsj). Indeed, the simple correlogram permit to identify the number of delay q of the model MA (q), while the partial correlogram allow to identify the number of delay p of the model AR (p). According to figure 3-7 the PACF decreases slowly and exponentially, whereas the examination of the partial correlation shows us that the series can be modeled by an MA (3).

**Table 6. AIC of the ARIMA processes generated from the transformed data in Jiyeh station**

Model ARIMA	(0,1,0)	(0,1,1)	(0,1,2)	(0,1,3)
AIC	-2694.024	-3077.457	-3405.406	-3431.559

In Table 6, it appears that the ARIMA (0,1,3) process model is the best adapted model to the data for Jiyeh station according to the AIC criterion. The following Table 8 contains all estimated parameters of the ARIMA (0,1,3) model.

**Table 7. Parameters of the model ARIMA(0,1,3) estimated for Jiyeh station**

Model	Coefficients		
	ma1	ma2	ma3
ARIMA(0,1,3)	-0.5423	-0.3218	-0.1113

The ARIMA (0,1,3) model has the following form with  $rj_t$  the residual:

$$(1 - B)^d y_t = c + (1 + \theta_1 B + \theta_2 B^2 + \dots + \theta_q B^q) \epsilon_t$$

$$J_t = J_{t-1} + rj_t - 0.5423rj_{t-1} - 0.321rj_{t-2} - 0.113rj_{t-3}$$

Thus, it will be necessary to ensure that the residuals of the estimated series are "white noise", that is the average equal to 0, and the variance is constant non-auto-correlated. Consequently, the stationarity of the series and the fact that the residuals be "white noise" constitute the two essential properties.

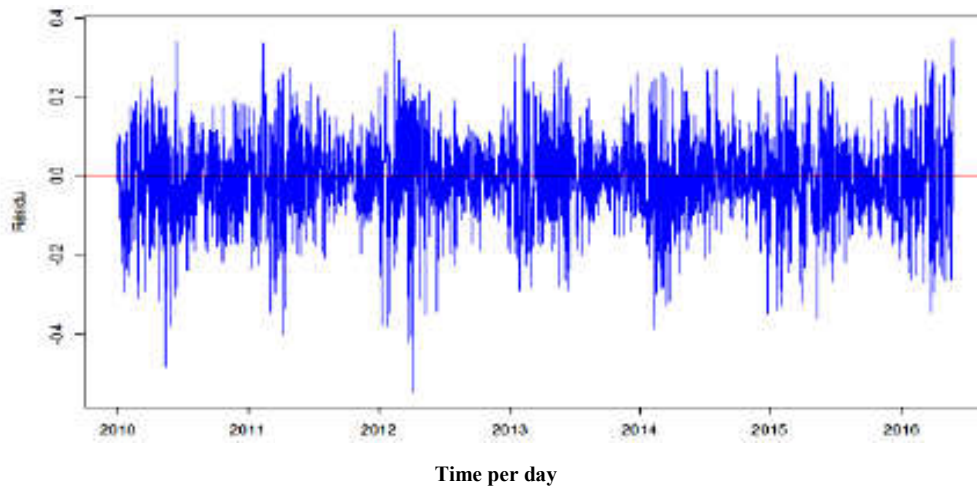


Figure 10. Representation of the residuals of the ARIMA (0,1,3) process for the Jiyeh station

Figure 10 shows that the series fluctuates around a constant average. The residues of the Jiyeh station of the ARIMA(0,1,3)model indicate that there exist a remarkable volatility, so it is necessary to testing the heteroscedasticity of these residues. Indeed, if the process is not stationary in variance, it is advisable to use, rather than an ARIMA process, but rather an ARIMA- (G) ARCH process in order to take into account the volatility and the non-linearity of the model.

Table 8. Heteroscedasticity test for the Jiyeh station

Lags	200	300	400
p-value	2.326e-11	2.199e-07	9.277e-06

According to the ARCH test applied to several lags, we find that p-value is close to zero. Therefore we reject the null hypothesis "Absence of an ARCH effect", so there exist a heteroscedasticity and it must be modeled from a GARCH (p, q)model.

*Choice of the GARCH(p,q) model*

Table 9. AIC of the GARCH processes generated from the square residue data ARIMA (0,1,3) from Jiyeh station

Model	c(0,1)	c(1,0)	c(1,1)	c(2,1)	c(1,2)	c(2,2)	c(0,2)	c(2,0)
AIC	-3520.43	-3464.22	-3687.84	-3684.54	-3562.1	-3633.88	-3538.83	-3459.75

Given the profile of autocorrelation and partial autocorrelation functions, we will choose the GARCH representation that best represents the dynamics of volatility. The best model is GARCH (1,1) having the smallest AIC value noted in Table 9.

Table 10. Parameters of the GARCH (1,1 ) model estimated at residue of the model ARIMA (0,1,3) of Jiyeh station

Model	a0	a1	b1
Value	0.000111	0.0534665	0.9392702

$$h(J)_t = 0.000111 + 0.0534665e(J)_{t-1}^2 + 0.9392702h(J)_{t-1}$$

Table 11. Test of heteroscedasticity effect on residues ARIMA (0,1,3) GARCH (1,1) - Jiyeh site

	100	200	300	Test	Comments	Heteroscedasticity
Residual ARIMA(0,1,3)	0	2.326e-11	2.199e-07	p-value<5%	Reject H0	exist
Residual GARCH(1,1)	0.2038	0.5703	0.5991	p-value>5%	Accept H0	Does not exist

The model chosen is validated. We apply the test of suitability on the residuals of the GARCH (1,1)model.

**Independence and normality of residues**

Table 12. Test of normality

Test	Jarque Berra	Kolmogorov-Sminrov	Agostino	
			Skweness	Kurtosis
P-value	0.0001057	0.7016	S=-3.3294	k=2.4477
Result (Threshold 5%)	Is not normal	Normal	Left asymmetry	

The hypothesis of the "white noise" residues of the GARCH (1,1) model of the Jiyeh site seems to be consolidated given the results obtained after the normality test is not well justified with a means equal to zero and variance equal to 0.99967. Finally, the same approach is applied for the other sites following the different steps previously developed for the Jiyeh station. The results are summarized in the following table, which present the synthesis of the ARIMA and GARCH process by station with the algebraic expressions of each process.

**Table 13. Summary of ARIMA processes**

Stations	ARIMA model	Residual	Analytic expressions
Jiyeh (J)	ARIMA(0,1,3)	rj	$J_t = J_{t-1} + rj_t - 0.5423rj_{t-1} - 0.3218rj_{t-2} - 0.1113rj_{t-3}$
Beirut(B)	ARIMA(0,1,3)	rb	$B_t = B_{t-1} + rb_t - 0.502rb_{t-1} - 0.326rb_{t-2} - 0.1459rb_{t-3}$
Batroun(Ba)	ARIMA(0,1,3)	rba	$Ba_t = Ba_{t-1} + rba_t - 0.4164rba_{t-1} - 0.3339rba_{t-2} - 0.1976rba_{t-3}$
Ouyoun Es Simen(Ouy)	ARIMA(0,1,2)	rOuy	$Ouy_t = Ouy_{t-1} + rOuy_t - 0.501rOuy_{t-1} - 0.477rOuy_{t-2}$
Sidon(Sid)	ARIMA(0,1,3)	rSid	$Sid_t = Sid_{t-1} + rSid_t - 0.5549rSid_{t-1} - 0.3244rSid_{t-2} - 0.0988rSid_{t-3}$
Tripoli(Tr)	ARIMA(3,0,0)	rTr	$Tr_t = Tr_{t-1} + rTr_t - 0.51rTr_{t-1} - 0.466rTr_{t-2}$
Tyre(Ty)	ARIMA(0,1,2)	rTy	$Ty_t = Ty_{t-1} + rTy_t - 0.5902rTy_{t-1} - 0.3895rTy_{t-2}$

In Table 13, there are four corresponding ARIMA(0,1,3) processes respectively at the stations of Jiyeh, Beirut, Batroun and Sidon and two ARIMA(0,1,2) processes for the sites of Ouyoun Es Simen and Tyre and finally an ARIMA (3,0,0) process for the station of Tripoli, where in all the residues of these models their exist a heteroscedasticity effect, so we have for each site a GARCH model which given in the following Table.

**Table 14. Summary of GARCH processes**

Stations	GARCH model	Analytic expressions
Jiyeh	GARCH(1,1)	$h(J)_t = 0.000111 + 0.0534665(J)_{t-1}^2 + 0.9392702h(J)_{t-1}$
Beirut	GARCH(1,1)	$h(B)_t = 0.0002407 + 0.0387836e(B)_{t-1}^2 + 0.9504509h(B)_{t-1}$
Batroun	GARCH(2,1)	$h(Ba)_t = 0.001285 + 0.064578e(Ba)_{t-1}^2 + 0.42751h(Ba)_{t-1} + 0.870577h(Ba)_{t-2}$
Ouyoun Es Simen	GARCH(1,1)	$h(Ouy)_t = 0.0008999 + 0.0590595e(Ouy)_{t-1}^2 + 0.9350131h(Ouy)_{t-1}$
Sidon	GARCH(2,1)	$h(Sid)_t = 0.00001566 + 0.09876e(Sid)_{t-1}^2 + 0.4552h(Sid)_{t-1} + 0.429h(Sid)_{t-2}$
Tripoli	GARCH(1,1)	$h(Tr)_t = 0.0009221 + 0.0344954e(Tr)_{t-1}^2 + 0.9478375h(Tr)_{t-1}$
Tyre	GARCH(1,1)	$h(Ty)_t = 0.00003172 + 0.07361e(Ty)_{t-1}^2 + 0.9208h(Ty)_{t-1}$

Table 14 summarizes the GARCH processes of each stations, five GARCH (1,1) models corresponding respectively to the Jiyeh, Beirut, Ouyoun Es Simen, Tripoli and Tyre stations and two GARCH (2,1) processes for the Batroun and Sidon stations.

**Table 15. Mean and standard deviation of innovations of the GARCH model**

Stations	Mean	Standard deviation	Normal
Jiyeh	0	0.99967	Not normal
Beirut	0	1.000566	Normal
Batroun	0	1.000189	Normal
Ouyoun Es Siman	0	1.000031	Not normal
Sidon	0	0.9977047	Not normal
Tripoli	0	1.00098	Normal
Tyre	0	0.9988447	Normal

**Table 16. Kendall rate between the residues of estimated GARCH processes**

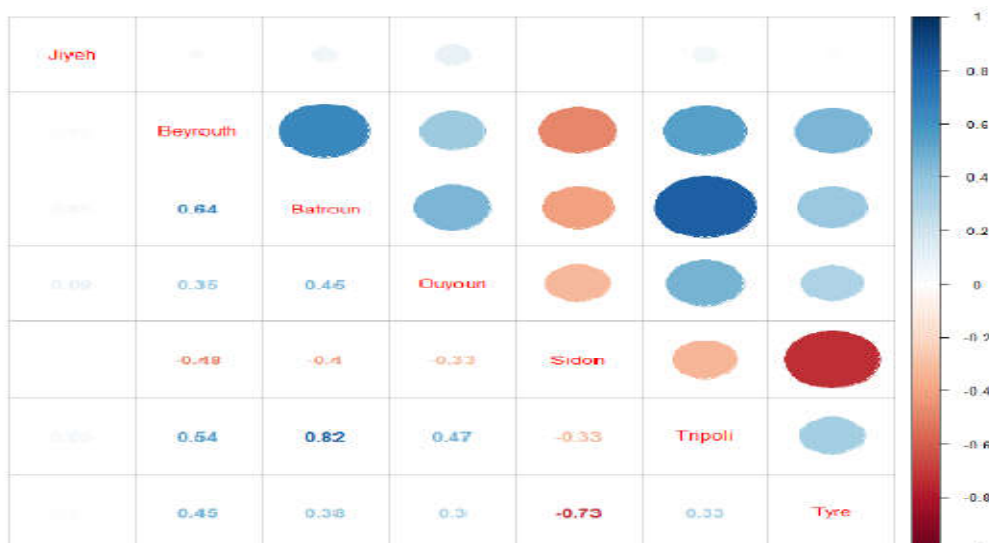


Table 15 shows that the innovations means of the GARCH model for the seven station equal to zero and the standard deviations closer to 1, but this does not reflect that these innovations are all Gaussian, such as in the innovations of the Jiyeh, Ouyoun Es

Simen and Sidon, where the other innovations of the stations of Beirut, Batroun Tripoli and Tire are Normal. For this reason it is necessary to apply in the following section the independence case by using the multivariate copulas. For the rest of this article, we generate a matrix called "Gvent". This matrix has seven columns and each column represents the innovations of the GARCH process at each site. The elements of the "Gvent" matrix represent the input data we use to analyze the dependence of the sites in the previous section.

**Copulas dependency stations**

In the previous section, we estimated seven stationary stochastic processes (GARCH) that fit the data of our seven stations (Jiyeh, Beirut, Batroun, Ouyoun EsSimen, Sidon, Tripoli and Tyre). Even if each station is modeled correctly, their joint behavior can be linked. To modelling the spatial dependency of the data, we adapt a multivariate model to the innovations of the time series. We estimate the correlations between the stations from the residuals of the estimated time series. This step will present the stations which have a geographical link according to the expression of the coefficient of correlation between the residuals. The main objective of this section is to identify the copula that describes the dependency structure between the correlated stations.

The stations that are positively linked to each other are: Batroun and Tripoli, Beirut and Batroun, Beirut and Tripoli, then Ouyoun Es Simen and Tripoli. The stations that are negatively related are Sidon and all other sites. First we define the using Copulas (Kalyan 2015):

- Gaussian copula:  $C(u_1, \dots, u_d) = \Phi_{\Sigma}(\Phi^{-1}(u_1), \Phi^{-1}(u_2), \dots, \Phi^{-1}(u_d))$ , where  $\Phi$  and  $\Phi_{\Sigma}$  are respectively the cumulative density function for normal distribution  $N(0,1), N(0_d, \Sigma)$ ;  $\Sigma$  represents the correlation matrix of the margins.
- Gumbel copula: we define the function  $\phi(u) = (-\ln u)^{\theta}$

$$C(u_1, \dots, u_d) = \left( \sum_{i=1}^d (-\ln u_i)^{\theta} \right)^{1/\theta}$$

Clayton copula: We define the generator function  $\phi(u) = u^{-\theta} - 1$ , with  $\theta \in (0, +\infty[$ .

$$C(u_1, \dots, u_d) = \left( \sum_{i=1}^d u_i^{-\theta} - d + 1 \right)^{-1/\theta}$$

Frank copula: We define the function  $\phi(u) = -\ln \frac{\exp(-\theta u) - 1}{\exp(-\theta) - 1}$ , with  $\theta \in (0, +\infty[$ .

$$C(u_1, \dots, u_d) = -\frac{1}{\theta} \ln \left[ 1 + \frac{1}{(e^{-\theta} - 1)^{d-1}} \prod_{i=1}^d (e^{-\theta u_i} - 1) \right]$$

Joe copula: we define the generator function  $\phi(u) = -\ln(1 - (1 - u)^{\theta})$  with  $\theta > 0$ .

$$C(u_1, \dots, u_d) = 1 - \left[ 1 - \prod_{i=1}^d (1 - (1 - u_i)^{\theta}) \right]^{\frac{1}{\theta}}$$

**DISCUSSION**

Now we can apply the test of suitability of copulas with Cramer-Von Mises and Kolmogorov-Smirnov.

**Table 17. Results of the copula fit test based on the Cramer-von Mises (Sn) and the Kolmogorov-Smirnov (Tn) with a p-value rejection threshold of 5%: Beirut and Batroun stations**

Copulas	$\theta_n$	$S_n$		$T_n$	
		Critical values	P-value	Critical values	P-value
Gaussian	0.845403	0.959516	0	1.926238	0
Clayton	3.575376	7.184857	0	4.750594	0
Gumbel	2.787688	0.062663	0.18	0.691599	0.17
Frank	9.146738	0.679684	0	1.372695	0
Joe	4.389817	18.30545	1	5.964256	1

First, according to the p-values of the Cramer-von Mises (Sn) and Kolmogorov-Smirnov (Tn) tests, the suitability of the Gaussian and Clayton and Frank copulas to the empirical copula of the innovations is not accepted at the 5% threshold where the families of Gumbel, and Joe are accepted at the 5% threshold. We note that the Gumbel copula is significantly better than the Joe copula, since its distance to the empirical copula is lower (2.7877 vs. 4.3897 for Joe's copula).

**Table 18. Results of the copula fit test based on the Cramer-von Mises (Sn) and the KolmogorovSmirnov (Tn) with a p-value rejection threshold of 5%: Tripoli and Batroun stations**

Copulas	$\theta_n$	$S_n$		$T_n$	
		Critical values	P-value	Critical values	P-value
Gaussian	0.958878	0.149869	0.08	0.830121	0.13
Clayton	8.916911	5.382757	0	4.24299	0
Gumbel	5.458455	0.050528	0.08	0.598721	0.21
Frank	20.04181	0.408273	0	1.126818	0
Joe	9.679711	18.30545	1	5.964256	1

According to the two tests Cramer-von Mises ( $S_n$ ) and Kolmogorov-Smirnov ( $T_n$ ) at the 5% threshold, we accept the suitability of the copulas of Gaussian and Gumbel and Joe to the empirical copula of the innovations and we note that the Gaussian copula is significantly better than the copula of Joe and Gumbel since the distance to the empirical copula is lower (0.958878 against 9.679711 for the copula of Joe and 5.458455 for the copula of Gumbel). We do not accept the suitability of the copula Clayton and Frank.

**Table 19. Results of the copula fit test based on the Cramer-von Mises ( $S_n$ ) and the Kolmogorov Smirnov ( $T_n$ ) with a p-value rejection threshold of 5%: Tripoli and Ouyoun Es Simen stations**

Copulas	$\theta_n$	$S_n$		$T_n$	
		Critical values	P-value	Critical values	P-value
Gaussian	0.670951	1.150859	0	1.781753	0
Clayton	1.761006	7.829876	0	4.791284	0
Gumbel	1.880503	0.438218	0	1.238366	0
Frank	5.186759	0.74405	0	1.397748	0
Joe	2.62665	18.30545	1	5.964256	1

It is noted in Table 19 that the values for the four copulas Gaussian, Clayton, Gumbel and Frank are smaller than threshold 5% in the two tests Cramer-von Mises ( $S_n$ ) and Kolmogorov-Smirnov ( $T_n$ ), so we do not accept the null hypothesis of the adequacy of the copulas these copulas with the empirical copula of the innovations on the contrary one accepts it for the copula of Joe.

**Table 20. Results of the copula fit test based on the Cramer-von Mises ( $S_n$ ) and the KolmogorovSmirnov ( $T_n$ ) with a p-value rejection threshold of 5%: Tripoli and Beirut stations**

Copulas	$\theta_n$	$S_n$		$T_n$	
		Critical values	P-value	Critical values	P-value
Gaussian	0.752693	1.088413	0	2.090288	0
Clayton	2.371501	7.264653	0	4.872366	0
Gumbel	2.185751	0.081679	0.11	0.65344	0.27
Frank	6.567275	0.863901	0	1.677575	0
Joe	3.215188	18.30545	1	5.964256	1

At the 5% threshold we accept the suitability of the Gumbel and Joe copulas with the empirical copula of innovations with p-values > 0.05 and we note that the Gumbel copula is significantly better than the Joe copula since its distance to Copula is lower (2.185751 against 3.215188 for the copula of Joe). We do not accept the null hypothesis for the Gaussian, Clayton and Frank copula according to the two tests Cramer-von Mises ( $S_n$ ) and Kolmogorov-Smirnov ( $T_n$ ).

In this section we studied the bivariate copulas which are strongly dependent and we test the fit of the copulas according to the tests of Cramer-von Mises ( $S_n$ ) and KolmogorovSmirnov ( $T_n$ ). But what interests us in this study is to find an intermediate model that requires few parameters, while guaranteeing a satisfactory fit quality to the innovations of the multivariate variables, for this we need in order to solve this problem, for this we can interested in future research to study the Copulas“vines” where the construction of copulas in vines is based on the decomposition of a multidimensional density using the bivariate conditionals copulas.

## REFERENCES

- Al Zohbi, G., P. Hendrick et P. Bouillard : Evaluation du potentiel d'énergie éolienne au Liban, *Revue des Energies Renouvelables* Vol. 17 N°1 (2014) 83 – 96.
- Allen, S. R., Hammond, G.P. and McManus, M.C., 2008. Energy analysis and environmental life-cycle assessment of a microwind turbine, *Proceedings of the Institute of Mechanical Engineering, Journal of Power and Energy, Part A, Vol 222, Special Issue Paper*, pp. 669-684.
- Benth, J. r. a., and Benth, F. E. 2010. Analysis and modelling of wind speed in New York. *Journal of Applied Statistics*, 37(6), 893 - 909.
- Box, G. E. P. and Cox, D. R. 1964. An analysis of transformations, *Journal of the Royal Statistical Society, Series B*, 26, 211-252.
- Dickey, D.A. W.A. Fuller, 1979. Distribution of the Estimators for Autoregressive Time Series with a Unit Root, *Journal of the American Statistical Association*, 74, pp. 427-31.
- Fthenakis, V.; Kim, H. C. 2009. "Land use and electricity generation: A life-cycle analysis". *Renewable and Sustainable Energy Reviews*. 13 (6–7): 1465.

- Harajli, H., E. Abou Jaoudeh, J. Obeid, W. Kodieh, M. Harajli, 2011. Integrating wind energy into the Lebanese electricity system; Preliminary analysis on capacity credit and economic performance, World Engineers' Convention 2011, September 4-9, Geneva.
- Kalyan Veeramachaneni, Alfredo Cuesta-Infante, Una-May O'Reilly, Copula Graphical Models for Wind Resource Estimation, 2015
- Kwiatkowski, D., P.C.B. Phillips, P. Schmidt, Y. Shin (1992): Testing the Null Hypothesis of Stationarity against the Alternative of a Unit Root, *Journal of Econometrics*, 54, pp. 159-178, North-Holland.
- Nicola Armaroli, Vincenzo Balzani, *Towards an electricity-powered world*. In: *Energy and Environmental Science* 4, 2011. 3193–3222, p. 3217
- Oliver Grothe et Julius Schieders, 2011. Spatial dependence in wind and optimal wind power allocation: a copula based analysis, May.
- Phillips, P.C.B., P. Perron, 1988. Testing for a Unit Root in Time Series Regression, *Biometrika*, 75, pp. 335- 346.

\*\*\*\*\*